Utilization of structural high entropy alloy for CO oxidation to CO_2

Anjali Sharma[a†], Nirmal Kumar Katiyar[b,c†], Arko Parui[d†], Rakesh Das[e], Abhishek Kumar Singh[d]*, Chandra Sekhar Tiwary[e*], , Sudhanshu Sharma[a*], Krishanu Biswas[b*]

[a]Department of Chemistry, Indian Institute of Technology Gandhinagar, Gandhinagar 382355, India

[b]Department of Materials Science and Engineering, Indian Institute of Technology Kanpur, Kanpur 208016, India

[c]School of Engineering, London South Bank University London, 103 Borough road, London SE10AA

[d]Materials Research Centre, Indian Institute of Science, Bangalore 560012, India

[e]Metallurgical and Materials Engineering, Indian Institute of Technology Kharagpur, Kharagpur 382355, India

*Corresponding authors, Email: abhishek@iisc.ac.in, ssharma@iitgn.ac.in, Chandra.tiwary@metal.iitkgp.ac, kbiswas@iitk.ac.in

†Equal Contribution

Abstract

The nanoengineered high entropy alloy (HEAs) catalysts have attracted the attention of the scientific community due to their exceptional characteristics; wide range of compositional tunability and the utilization of low-cost transition metals. During various electrochemical reactions, the oxidation of carbon-mono-oxide (CO) is an intermediate and it acts as a poison to reduce the efficiency of the reactions. A nanocrystalline HEA catalyst (CoFeNiGaZn) is prepared by easily scalable cast-cum-crush method, providing pristine catalyst surfaces. It is capable of catalyzing the CO-oxidation to CO_2 with high conversion efficiency (99.8%). DFT calculations show that the high activity of the HEA can be attributed to the presence of a considerable amount of filled states of d_{xz} and d_{yz} orbital near the Fermi level for Ni atoms over the surface. Due to the favourable transfer of electrons from this orbital to the LUMO of reactant molecules, the endothermicity of the rate-determining step is 1.13 eV.

Keywords: Electro-oxidation; High entropy alloy, Catalyst, Low cost, DFT, Transition metals

The engineered nano or atomic scale catalysts have revolutionized the domain of catalysis by providing high selectivity and activity with long term stability, raising hope for sustainability for industrials applications [1, 2]. However, noble metal catalysts, commonly utilized are too precious to make them viable for commercial operation. Therefore, nanoengineered catalysts using low-cost elements (transition metal elements), which must be endowed with high stability and efficiency, are the need of the hour. In this regard, different types of materials are under active consideration as well as investigation, revolutionizing the catalytic science to meet the novel requirements, including graphene for HER reaction [3], electronic waste as a catalyst for water splitting[4], carbon dots for ORR and OER reactions [5] etc. However, limitations exist, such as the yield of the catalyst preparation, lack of efficiency, and lower selectivity, which requires the design and development of new catalysts

A new concept called entropy stabilized multicomponent alloys, popularly known as high entropy alloys has emerged and reported to be successful in design of novel catalysts for variety of reactions [6]. The five or more elements are mixed in equiatomic or near equiatomic ratio to form single-phase alloys, which has recently been used to design novel catalysts [7, 8]. They have shown tremendous potential due to their vast compositional space comprising almost all the metallic elements in the periodic table, allowing us to tune the chemistry and surface microstructure and provide the unlimited scope of design new multipurpose catalysts. Among the low-cost metals available in the periodic table, the alloys made of 3d-transition metals (TMs) are considered to be the best candidates for the nanoengineered HEA catalysts [6]. The four-core effects of HEAs impart exceptional properties; high entropy providing the single-phase stabilization, sluggish diffusion imparting long-term stability, cocktail effect altering their d-band centre with respect to Fermi energy level, and the lattice distortion modifying energy levels of

free electrons[9-11]. Therefore, the high entropy alloys (HEAs) are expected to provide an active catalyst because a single-compositional alloy can exhibit multiple reactions due to multi-elemental bonds dangling over the surface with a unique surface electronic structure favourable for the adsorption[12]. This allows the design gamut of the chemistry of high entropy catalysts with different elements for their electrochemical responses. This includes degradation of azo dyes using AlCoCrTiZn HEA catalyst[13], converting CO_2 into highly reduced hydrocarbon (CH_4, CH_3OH) using AgAuPdPtCu HEA catalyst [14], formic acid and methanol to hydrogen fuel[15]. The NH_3 decomposition using high entropy alloy (CoMoFeNiCu) was 20 times higher than the pure Ru catalyst[16]. CO oxidation reaction, one of the important yet simple exhaust treatment reactions, has not extensively been studied on the high entropy catalysts. Preferential CO oxidation is important to purify hydrogen gas where CO concentration of lower than 5 ppm is required [17]. Supported Pt catalyst is the most widely used one for this reaction although the cobalt-based catalysts exist, providing ultra-low temperature activity [18, 19]. Among various materials used for this reaction are supported metal oxides, perovskite, spinels, substituted metal oxides etc [20-23]. Among the emerging class of materials, HEAs can possibly outperform previously known catalysts for CO oxidation reaction. However, the magic chemistry is still unknown as a low volume of work exists for CO oxidation reaction on HEAs [24]. In fact, a basic kinetic investigation is not reported so far, which can, in principle lead to a fair comparison of HEAs with the conventional catalysts. In this work, we have explored the CO oxidation activity on low cost easily scalable *CoFeZnNiGa* HEA nanoparticles. The kinetic parameters have been estimated and compared with the other known catalysts in the literature. The nanocrystalline *CoFeZnNiGa* HEAs has been prepared by the method of cast-and-crushing, involving cryomilling of the cast alloy ingot at extremely low temperature [25, 26]. Therefore,

the surface of the catalyst remains native or uncapped due to low temperature milling, making it viable for catalytic applications [25, 27]. Further DFT calculations were done to find the active site over the HEA surface along with the probable mechanism, where mainly the effect of suitable orbital overlap among the HEA and reactant molecule was considered.

Results and discussion

Figure 1(a) shows the schematic representation of the recipe of synthesis and nature of atomic arrangement on the HEA nanoparticle; each constituent of HEA is present on surface of the nanoparticle, allowing adsorbate molecule to land over the surface of the nanoparticles and turn to CO_2. A unique recipe has been applied to prepare a five-element HEA catalyst using low-cost materials transition elements for this purpose; Fe, Ni, Co, Ga and Zn. The elements were melted together in an argon environment to obtain an ingot and then milled at extremely low temperatures (-123 K) to avoid oxidation and contamination of the nanocrystalline HEA. The XRD pattern (Figure 1b) reveals single-phase FCC nanoparticles are being synthesized by this route. The size and shape of as-prepared nanoparticles were obtained from bright-field TEM micrograph (Figure 1(c)) and the average size is found to be ~12 ±3 nm. Their surface is pristine, as shown in the HRTEM image of a nanoparticle in Figure (d). It is to be noted that there are five different elements in single HEA nanoparticle, and therefore, the homogeneity (element distribution) has been confirmed by elemental mapping using EDS attached to the TEM. Figure 1(f) shows elemental maps for a nanoparticle, revealing that all elements are homogeneously distributed in the single-phase materials.

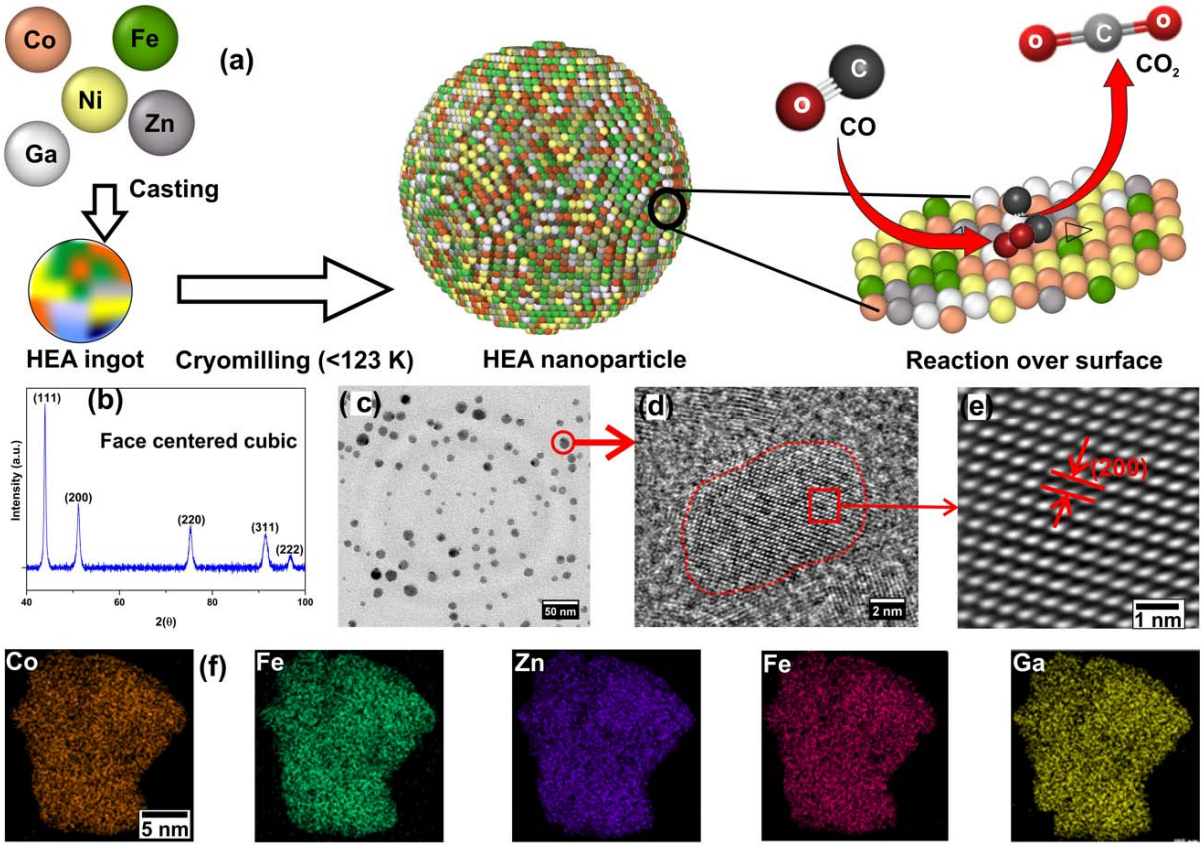

Figure 1: (a) Schematic of recipe for preparation of HEA nanoparticles and CO oxidation over the HEA nanoparticle surface, **(b)** X-ray diffraction pattern of HEA nanoparticles, **(c) B**right field TEM micrograph of the nanoparticles, **(d)** HRTEM image of a single nanoparticle, **(e)** FFT filtered image corresponding to image (d),(f)EDS elemental maps of a single nanoparticle.

The HEA nanoparticles are further investigated for heterogeneous gas-solid reaction in the unsupported state. The CO-oxidation reaction is carried out under stoichiometry conditions, the details of gas mixture containing 10% carbon monoxide, 10% Oxygen and remaining Nitrogen. The conversion profile of CO over *CoFeZnNiGa* as a function of the temperature is shown in Figure 2(a). All profiles are recorded in the temperature range from room temperature to 400 °C and using the CO/O_2 ratio of 2:1.

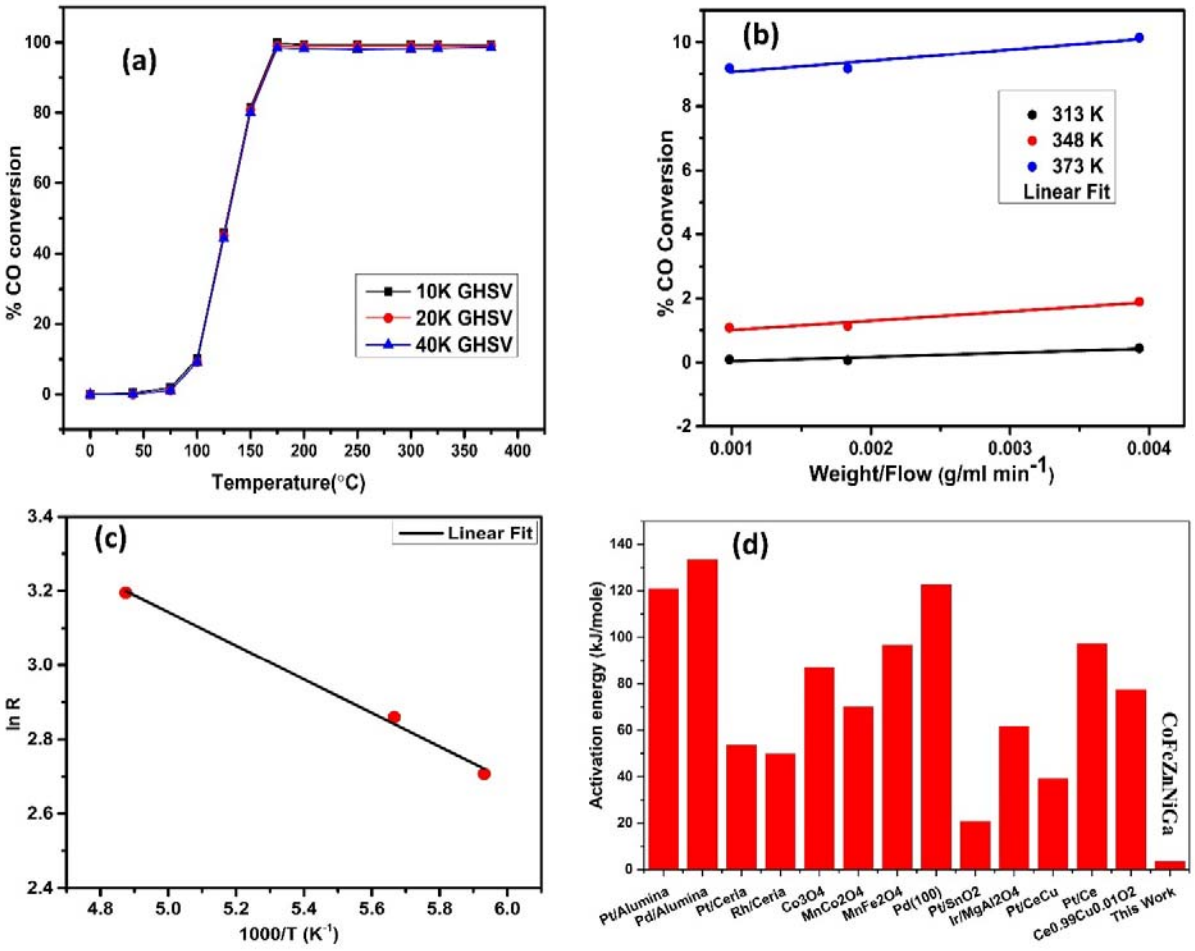

Figure 2: (a) Percentage CO conversions of CO + O_2 reaction at different GHSV for *CoFeZnNiGa*, **(b)** Percentage CO Conversion vs *W/F* at 313K, 348K and 373K for different GHSV (descending from left to right) at atmospheric pressure. The amount of the catalyst for all cases is fixed at 55 mg, **(c)** Arrhenius plot for CO+O_2 reaction over CoFeZnNiGa catalyst. The reported values are for steady-state rates measured at temperatures of 313, 348, and 373K with a total conversion of CO below 12%, **(d)** Activation energy for different catalyst materials of CO oxidation reaction (data collected from the literature).

The dependence of CO conversion on the flow rates was studied and the results are shown in Figure 2(b). As the space velocity was increased from10,000 – 40,000 h^{-1}(GHSV), no effect was observed on the CO conversion profile and temperature. It concludes that external diffusion (mass transfer) has a limited role on the catalytic activity. This is partially due to the fact that

HEA nanoparticles do not contain any macroscopic porosity (as its free-standing nature). Maximum % conversion of CO over CoFeZnNiGa was found out to be 99.8% at 175^0Cat 10,000 h^{-1} GHSV. The rate of CO oxidation reaction was also calculated at various temperatures from the slope of the curve (*W/F*) with the molar conversion of CO (Figure 2c). Here, *W* is the weight of the catalyst, and *F* is the flow rate of CO in sccm [19, 28, 29]. Rates of the reaction w.r.t weight at temperatures 313K, 348K, 373K were found out to be 2.38, 5.26, 6.39 µmol/g/sec, respectively. Activation energy was found to be 3.761 kJ/mol, which is the lowest among the materials well-known in literature (Figure 2d). Cleary, the HEA catalyst is highly active for the CO oxidation reaction.

To shed light on the probable mechanism and active sites for reaction, density functional theory (DFT) calculations were performed. In the first step, FCC bulk structure of Ni was taken from Materials Project [30] to generate the FCC-HEA surface. Optimized lattice parameters are (a=b=c=3.52 Å) which is in good agreement with previous report [31]. The (111) facet was selected for DFT calculations, as it shows the most prominent pick in the XRD pattern. It was generally believed that for CO oxidation ($CO + O \rightarrow CO_2$), O_2 adsorption takes place on the surface. Its dissociation follows this on transition metals as O_2 can easily dissociate on all transition metals at room temperature[32]. Therefore, the reaction follows Langmuir-Hinshelwood mechanism, and the elementary steps involved in the reactions are (i) CO adsorption on the surface, (ii) O_2 dissociation into O adatoms on surfaces, and (iii) $CO + O \rightarrow CO_2$ reaction on the surface. Accordingly, the reaction rate depends on the favourable activation of both adsorbed CO and O_2. This occurs by the transfer of electrons from the Fermi level of *CoFeZnNiGa* alloy surface to the lowest unoccupied molecular orbital (LUMO) of CO or O_2, which are antibonding in nature for the both [33, 34].

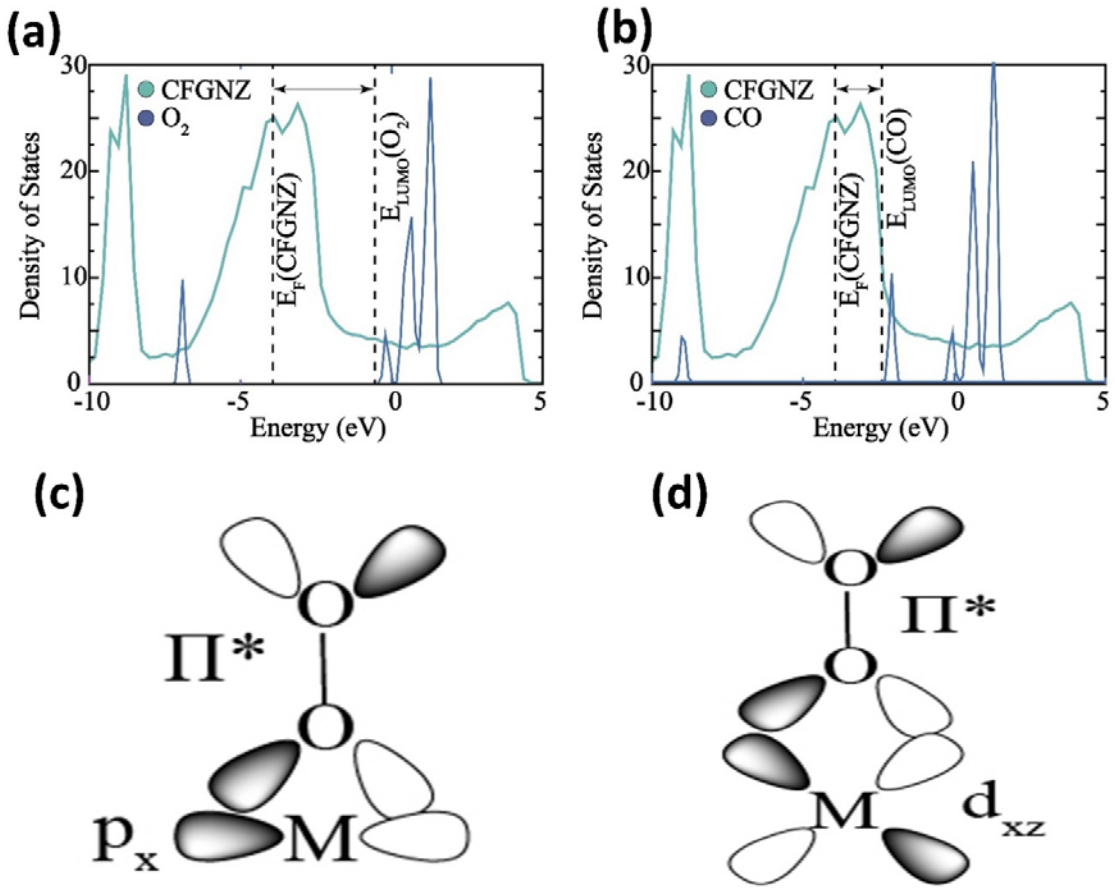

Figure 3: Comparison of Fermi level energy of *CoFeZnNiGa* alloy with energy of LUMO of **(a)** O_2 and **(b)** CO, **(c)** Interaction of Π* orbital of O_2 with the p_x and **(d)** d_{xz} orbital of metals on the surface.

To understand the factors contributing to the initial adsorption of reactant molecules, energies of Fermi level (E_F) of surface of the *CoFeZnNiGa* alloy and LUMO (E_{LUMO}) of CO and O_2 were compared (Figure 3(a,b)). E_F of metallic *CoFeZnNiGa* alloy surface is -4.29 eV, which is energetically lower from E_{LUMO} (-0.24 eV) of O_2 than E_{LUMO} (-2.71 eV) of CO. Therefore, electron transfer from the catalytic surface to O_2 is more difficult than to CO. Adsorption of CO on the surface depletes the electron availability for the activation of O_2. Hence, the adsorption and the dissociation of O_2 were considered to be the first step followed by adsorption of CO. To

understand the most favourable adsorption sites of O_2 and CO, their orbital interaction with the surface was considered. For both O_2 and CO, the LUMO is Π* orbital and hence more prone to interact with the p_x or p_y orbitals of Ga and d_{xz} or d_{yz} orbitals of Co, Ni, Fe, Zn atoms on the surface Figure 3(c,d). Therefore, a particular atom having more filled states contributed from previously considered orbitals near the Fermi level has more potentiality to transfer the electron for adsorption and activation of O_2 and CO. Being more stabilized on the hollow sites, for the adsorption of O_2, the average value of the filled states within 1 eV near the Fermi level of different hollow sites on the surface was calculated. A particular hollow site containing only Ni atoms came out to be the most suitable adsorption site according to the criteria; Figure 4(a). Optimized structure of adsorbed O_2 on the chosen hollow site leads to the spontaneous formation of 2O* adsorbed on different sites, indicating high activity of *CoFeZnNiGa* alloy surface. Hence, the adsorption of only one O* was considered as stability of this particular intermediate determines the feasibility of the first elementary step.

In the next step, a similar exercise was done to find out the most suitable adsorption site for CO on the surface containing O*. A particular hollow site containing only Ni-atoms next to the adsorption sites of O maintained the aforementioned criteria (Figure 4(b). After the adsorption of CO, in the neighbouring O site on the *CoFeZnNiGa* alloy surface, the structure was optimized. The free energy diagram was calculated to understand the rate-determining step in the considered mechanistic pathway (Figure 5). Adsorption of O on the surface is less endothermic (0.56 eV) as compared to that of (1.13 eV) of adsorption of CO. This is obvious as initially adsorbed O pulls surface electrons, making the stabilization CO difficult. Desorption of CO_2 from the surface is highly exothermic, putting *CoFeZnNiGa* alloy surface forward as an active catalyst for CO oxidation reaction.

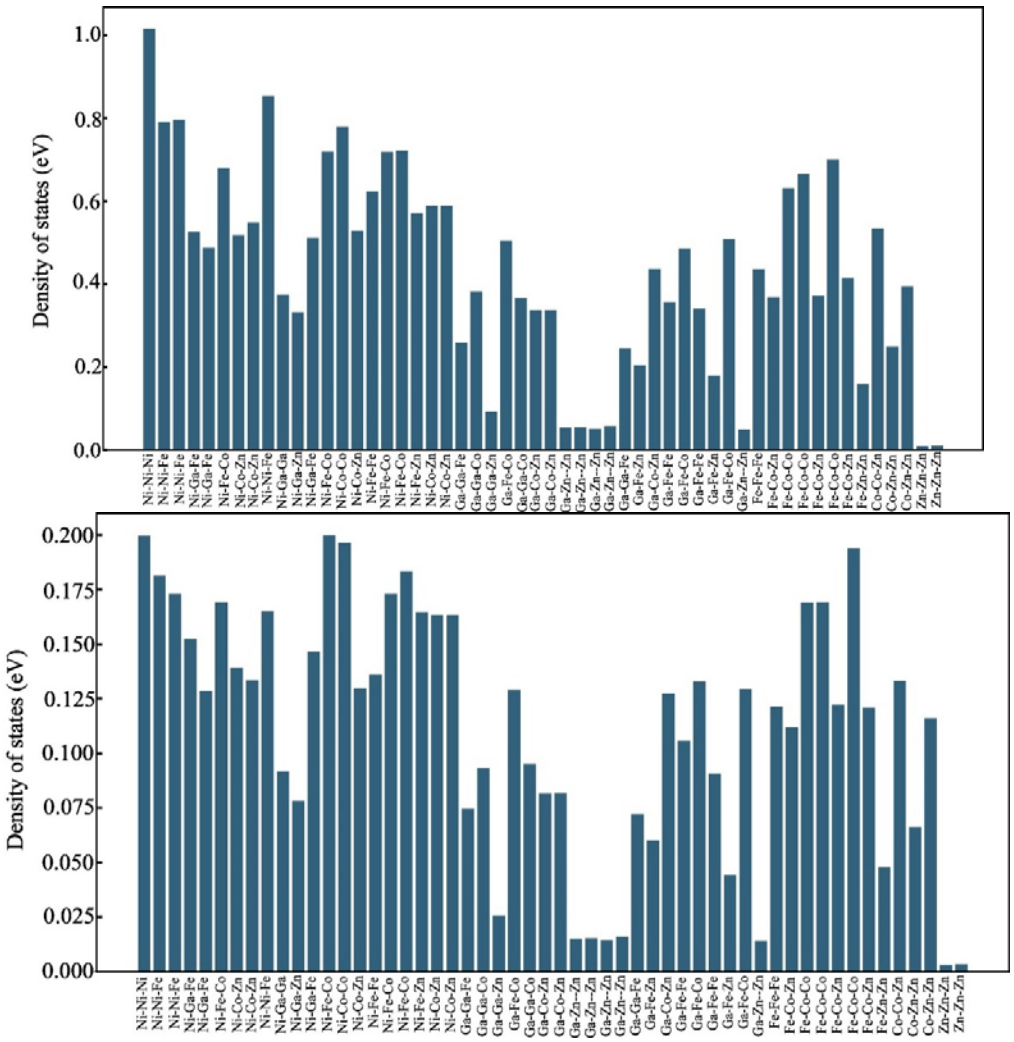

Figure 4:(a) Average value of density of states of the hollow sites on the *CoFeZnNiGa* alloy surface contributed by p_x and p_y orbital for Ga atom and d_{xz} and d_{yz} orbital for Co, Fe, Ni, Zn atoms within 1 eV near the fermi level **(b)** Average value of density of states of the hollow sites on the *CoFeZnNiGa* alloy surface with adsorbed O* contributed by p_x and p_y orbital for Ga atom and d_{xz} and d_{yz} orbital for Co, Fe, Ni, Zn atoms within 1 eV near the Fermi level.

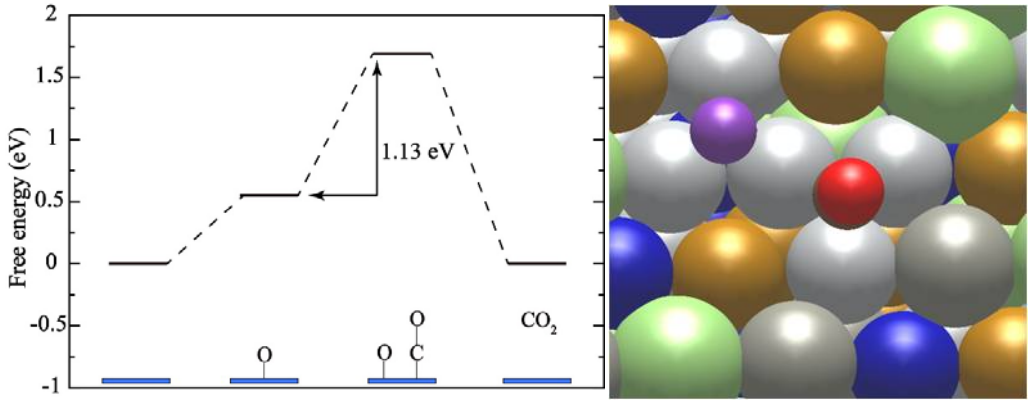

Figure 5: **(a)** Free energy diagram of CO oxidation over *CoFeZnNi*Ga alloy surface, **(b)** CO and O adsorbed over the *CoFeZnNiGa* alloy surface. Purple ball represents O and Red call represents the O of CO.

Conclusions

Catalytic CO oxidation over low-cost novel *CoFeZnNiGa* HEA nanoparticles, synthesized by cast-cum-crush method was carried out in the presence of the feed oxygen. The conversion and selectivity curves of CO oxidation at different GHSV indicate a maximum CO conversion of 99.8% was achieved at 175°C and 10,000 GHSV. Activation energy was found to be 3.8 kJ/mol, which is the lowest among the well-studied catalysts in the literature. Rates of the reaction at temperature 313k, 348k, 373k are found out to be 2.38, 5.26, 6.39 μmol/g/sec, respectively. DFT calculations showed the high activity of Ni hollow sites for CO conversion where the rate-determining step is the adsorption of CO having endothermicity of 1.13 eV at the adjacent site of adsorbed O on (111)-oriented surface of the HEA. This is because the d_{xz} and d_{yz} orbitals of the active Ni-atoms contain many filled states near the Fermi level, which can easily transfer.

Materials and method

The pure metal elements were purchased from the Alfa Aesar with 99.99% purity in chips. The nanocrystalline high entropy alloy was prepared by casting-cum-comminution method (CCC); details can be seen in previous studies [25, 27]. All five elements were melted in equiatomic ratio under argon environment by arc melting. After multiple melting, an ingot was obtained with a single-phase high entropy alloy. The ingot was parted into small pieces and cryomilled for 7 hours to obtain the nanocrystalline HEA. The extremely low temperature (<123 K) suppress the oxidation and cold welding and provide the free nanoparticles with a pristine surface [25, 27].

Catalytic activity test

The catalytic activities test of *CoFeZnNiGa* for CO oxidation reaction was carried out in packed bed reactor. A powdered sample was mixed with catalytically inert silica to improve the flow characteristics of the reactants and the heat distribution in the catalyst. The catalyst bed was loaded with 110 mg of the sample in a tubular quartz tube (25 cm length and 4 mm internal diameter). Both the ends were plugged with the help of quartz wool. This tube was introduced into a tubular furnace where the temperature is controlled by a PID controller. For the CO oxidation reaction, carbon monoxide (10% CO+ 90% N_2) and Oxygen (10% O_2 + 90% N_2) were used as the reactants, and additional UHP N_2 was used as the carrier gas. In an experiment, the reaction mixture was passed continuously through the catalyst bed, and the temperature was increased from RT to 400 °C. The ratio of the reactants (CO/ O_2) was maintained as 2:1 and the reactions were performed by varying the space velocity from 10,000 to 40,000 h^{-1}. The feed gas flow rates of O_2 (7sccm) & CO (14sccm) were 21ml/min. (10,000 GHSV), which were controlled by mass flow controllers (ALICAT MC Series). A K-type thermocouple was used to measure the catalyst bed temperature. The outlet gas from the reactor was analyzed by a gas

chromatograph (CIC Baroda) using both a Flame Ionization Detector (FID) and a Thermal Conductivity Detector (TCD). The columns used in the GC were PORAPAK-N and PORAPAK-Q. All the experiments were carried out at atmospheric pressure. The amount of the catalyst used was 110 mg (55mg catalyst+55mg silica).

% Conversion (X) of CO was calculated using the following equations [35] :

$$X(CO) = \frac{(CO_{in} - CO_{out})}{CO_{in}} \times 100$$

First, CO was allowed to adsorb on samples at a flow rate of 15ml/min for 30 min at room temperature. The catalyst was then flushed with nitrogen for 30 min at room temperature to remove the gas phase and weakly adsorbed CO. Finally, the catalyst was heated from 25 °C to 400 °C at a constant heating rate of 10°C/min in the presence of nitrogen and desorbed CO and CO_2 was monitored. For the quantification of Conversion of CO, O_2 and the reaction product, calibration of GC was done. A calibration experiment was performed in which the standard gas mixture (CO, CO_2, H_2, N_2) was used. 1 ml of this calibration standard gas was injected in GC, and the areas of different peaks of the gases were noted for the known concentration of the gases. These values were used to find out the moles of each gas in CO oxidation reaction.

Simulation methodology

Density functional theory (DFT) were done with "Vienna ab initio simulations (VASP)" package [36]. The Electron-ion interactions were described using all-electron projector augmented wave pseudopotentials, and "Perdew-Bruke-Ernzehof (PBE)" "generalized gradient approximation (GGA)" was used to approximate the electronic exchange and correlations[37]. The plane-wave kinetic energy cut off of 520 eV was used. All the structures were optimized using a conjugate gradient scheme until the energies, and the components of forces reached 10-5 eV and 0.01 eV

Å-1. A vacuum of 10 Å was added in the z-direction to prevent interactions between the periodic images. The Brillouin zone were sampled with 2*4*1 Monkhorst-Pack. DOS calculations for surfaces were performed by sampling the Brillouin zone with 4×8×1 Monkhorst-Pack. Fermi level of CoFeZnNiGa was calculated with respect the local potential. All the calculations were spin-polarized.

Competing interests:

The authors declare no competing interests.

Notes

The authors declare no competing financial interest.

Acknowledgments

The authors would like to thank SERB-DST for the financial support to carry out this research. We would also like to thank the Imaging center facilities at the Indian Institute of Technology Kanpur for TEM imaging.

Reference

[1] R.I. Masel, Z. Liu, H. Yang, J.J. Kaczur, D. Carrillo, S. Ren, D. Salvatore, C.P. Berlinguette, An industrial perspective on catalysts for low-temperature CO2 electrolysis, Nat. Nanotechnol. 16 (2021) 118-128, https://doi.org/10.1038/s41565-020-00823-x.

[2] Nanoscale engineering for sustainable catalysis, Nat. Nanotechnol. 16 (2021) 117-117, https://doi.org/10.1038/s41565-021-00862-y.

[3] A. García-Miranda Ferrari, D.A.C. Brownson, C.E. Banks, Investigating the Integrity of Graphene towards the Electrochemical Hydrogen Evolution Reaction (HER), Sci. Rep. 9 (2019) 15961, https://doi.org/10.1038/s41598-019-52463-4.

[4] V.R. Jothi, R. Bose, H. Rajan, C. Jung, S.C. Yi, Harvesting Electronic Waste for the Development of Highly Efficient Eco-Design Electrodes for Electrocatalytic Water Splitting, Adv. Eng. Mater. 8 (2018) 1802615, https://doi.org/10.1002/aenm.201802615.

[5] J. Liu, S. Zhao, C. Li, M. Yang, Y. Yang, Y. Liu, Y. Lifshitz, S.-T. Lee, Z. Kang, Carbon Nanodot Surface Modifications Initiate Highly Efficient, Stable Catalysts for Both Oxygen Evolution and Reduction Reactions, Adv. Eng. Mater. 6 (2016) 1502039, https://doi.org/10.1002/aenm.201502039.

[6] N. Kumar Katiyar, K. Biswas, J.-W. Yeh, S. Sharma, C. Sekhar Tiwary, A perspective on the catalysis using the high entropy alloys, Nano Energy 88 (2021) 106261, https://doi.org/10.1016/j.nanoen.2021.106261.

[7] B. Cantor, Multicomponent high-entropy Cantor alloys, Progress in Materials Science (2020) 100754, https://doi.org/10.1016/j.pmatsci.2020.100754.

[8] B. Cantor, I.T.H. Chang, P. Knight, A.J.B. Vincent, Microstructural development in equiatomic multicomponent alloys, Mater. Sci. Engg. A 375-377 (2004) 213-218, https://doi.org/10.1016/j.msea.2003.10.257.

[9] M.T. Gorzkowski, A. Lewera, Probing the Limits of d-Band Center Theory: Electronic and Electrocatalytic Properties of Pd-Shell–Pt-Core Nanoparticles, J. Phy. Chem. C 119 (2015) 18389-18395, 10.1021/acs.jpcc.5b05302.

[10] E.P. George, D. Raabe, R.O. Ritchie, High-entropy alloys, Nat. Rev. Mater. 4 (2019) 515-534, https://doi.org/10.1038/s41578-019-0121-4.

[11] E.J. Pickering, N.G. Jones, High-entropy alloys: a critical assessment of their founding principles and future prospects, Int. Mater. Rev. 61 (2016) 183-202, https://doi.org/10.1080/09506608.2016.1180020.

[12] Y. Sun, S. Dai, High-entropy materials for catalysis: A new frontier, Sci. Adv, 7 (2021) eabg1600, https://doi.org/10.1126/sciadv.abg1600.

[13] Z.Y. Lv, X.J. Liu, B. Jia, H. Wang, Y. Wu, Z.P. Lu, Development of a novel high-entropy alloy with eminent efficiency of degrading azo dye solutions, Sci. Rep. 6 (2016) 34213, https://doi.org/10.1038/srep34213.

[14] S. Nellaiappan, N.K. Katiyar, R. Kumar, A. Parui, K.D. Malviya, K.G. Pradeep, A.K. Singh, S. Sharma, C.S. Tiwary, K. Biswas, High-Entropy Alloys as Catalysts for the CO_2 and CO Reduction Reactions: Experimental Realization, ACS Catal. 10 (2020) 3658-3663, https://doi.org/10.1021/acscatal.9b04302.

[15] N.K. Katiyar, S. Nellaiappan, R. Kumar, K.D. Malviya, K.G. Pradeep, A.K. Singh, S. Sharma, C.S. Tiwary, K. Biswas, Formic acid and methanol electro-oxidation and counter

hydrogen production using nano high entropy catalyst, Mater. Today Eng. 16 (2020) 100393, https://doi.org/10.1016/j.mtener.2020.100393.

[16] P. Xie, Y. Yao, Z. Huang, Z. Liu, J. Zhang, T. Li, G. Wang, R. Shahbazian-Yassar, L. Hu, C. Wang, Highly efficient decomposition of ammonia using high-entropy alloy catalysts, Nat. Commun., 10 (2019) 4011, https://doi.org/10.1038/s41467-019-11848-9.

[17] S. Sharma, A. Gupta, M.S. Hegde, Pt2+ Dispersed in Ce0.83Ti0.15O2−δ: Significant Improvement in PROX Activity by Ti Substitution in CeO2 in Hydrogen Rich Stream, Catalysis Letters 134 (2010) 330-336, https://doi.org/10.1007/s10562-009-0249-8.

[18] T. Baidya, T. Murayama, S. Nellaiappan, N.K. Katiyar, P. Bera, O. Safonova, M. Lin, K.R. Priolkar, S. Kundu, B. Srinivasa Rao, P. Steiger, S. Sharma, K. Biswas, S.K. Pradhan, N. Lingaiah, K.D. Malviya, M. Haruta, Ultra-Low-Temperature CO Oxidation Activity of Octahedral Site Cobalt Species in Co3O4 Based Catalysts: Unravelling the Origin of the Unique Catalytic Property, J. Phy. Chem. C 123 (2019) 19557-19571, https://doi.org/10.1021/acs.jpcc.9b04136.

[19] A. Bisht, A. Sihag, A. Satyaprasad, S.S. Mallajosyala, S. Sharma, Pt Metal Supported and Pt4+ Doped La1−xSrxCoO3: Non-performance of Pt4+ and Reactivity Differences with Pt Metal, Catalysis Letters 148 (2018) 1965-1977, https://doi.org/10.1007/s10562-018-2408-2.

[20] H.-J. Freund, G. Meijer, M. Scheffler, R. Schlögl, M. Wolf, CO Oxidation as a Prototypical Reaction for Heterogeneous Processes, Angew. Chem. Int. Ed. 50 (2011) 10064-10094, https://doi.org/10.1002/anie.201101378.

[21] R. Prasad, P. Singh, A Review on CO Oxidation Over Copper Chromite Catalyst, Catalysis Reviews 54 (2012) 224-279, https://doi.org/10.1080/01614940.2012.648494.

[22] W. Yang, R. Zhang, B. Chen, N. Bion, D. Duprez, S. Royer, Activity of perovskite-type mixed oxides for the low-temperature CO oxidation: Evidence of oxygen species participation from the solid, J. Catal. 295 (2012) 45-58, https://doi.org/10.1016/j.jcat.2012.07.022.

[23] G. Fortunato, H.R. Oswald, A. Reller, Spinel-type oxide catalysts for low temperature CO oxidation generated by use of an ultrasonic aerosol pyrolysis process, J. Mater. Chem. 11 (2001) 905-911, https://doi.org/10.1039/B007306G.

[24] H.-J. Qiu, G. Fang, Y. Wen, P. Liu, G. Xie, X. Liu, S. Sun, Nanoporous high-entropy alloys for highly stable and efficient catalysts, J. Mater. Chem. A 7 (2019) 6499-6506, https://doi.org/10.1039/C9TA00505F.

[25] N. Kumar, C.S. Tiwary, K. Biswas, Preparation of nanocrystalline high-entropy alloys via cryomilling of cast ingots, J. Mater. Sci. 53 (2018) 13411-13423, https://doi.org/10.1007/s10853-018-2485-z.

[26] N.K. Katiyar, K. Biswas, C.S. Tiwary, Cryomilling as environmentally friendly synthesis route to prepare nanomaterials, Int. Mater. Rev. (2020) 1-40, https://doi.org/10.1080/09506608.2020.1825175.

[27] N.K. Katiyar, K. Biswas, C.S. Tiwary, L.D. Machado, R.K. Gupta, Stabilization of a Highly Concentrated Colloidal Suspension of Pristine Metallic Nanoparticles, Langmuir 35 (2019) 2668-2673, https://doi.org/10.1021/acs.langmuir.8b03401.

[28] J.A. Rodriguez, P. Liu, D.J. Stacchiola, S.D. Senanayake, M.G. White, J.G. Chen, Hydrogenation of CO2 to Methanol: Importance of Metal–Oxide and Metal–Carbide Interfaces in the Activation of CO2, ACS Catal. 5 (2015) 6696-6706, https://doi.org/10.1021/acscatal.5b01755.

[29] Y. Liu, H. Dai, J. Deng, X. Li, Y. Wang, H. Arandiyan, S. Xie, H. Yang, G. Guo, Au/3DOM La0.6Sr0.4MnO3: Highly active nanocatalysts for the oxidation of carbon monoxide and toluene, J. Catal. 305 (2013) 146-153, https://doi.org/10.1016/j.jcat.2013.04.025.

[30] A. Jain, S.P. Ong, G. Hautier, W. Chen, W.D. Richards, S. Dacek, S. Cholia, D. Gunter, D. Skinner, G. Ceder, K.A. Persson, Commentary: The Materials Project: A materials genome approach to accelerating materials innovation, APL Materials 1 (2013) 011002, https://doi.org/10.1063/1.4812323.

[31] D.R. Lide, CRC Handbook of Chemistry and Physics, 84th Edition, Taylor & Francis2003.

[32] X.-Q. Gong, R. Raval, P. Hu, General Insight into CO Oxidation: A Density Functional Theory Study of the Reaction Mechanism on Platinum Oxides, Phys. Rev. Lett. 93 (2004) 106104, https://doi.org/10.1103/PhysRevLett.93.106104.

[33] C.C. Romão, W.A. Blättler, J.D. Seixas, G.J.L. Bernardes, Developing drug molecules for therapy with carbon monoxide, Chem. Soc. Rev. 41 (2012) 3571-3583, https://doi.org/10.1039/C2CS15317C.

[34] W. Cai, X. Zhao, C. Liu, W. Xing, J. Zhang, 2 - Electrode Kinetics of Electron-Transfer Reaction and Reactant Transport in Electrolyte Solution, in: W. Xing, G. Yin, J. Zhang (Eds.), Rotating Electrode Methods and Oxygen Reduction Electrocatalysts, Elsevier, Amsterdam, 2014, pp. 33-65.

[35] M.M. Jaffar, M.A. Nahil, P.T. Williams, Parametric Study of CO2 Methanation for Synthetic Natural Gas Production, Energy Technol. 7 (2019) 1900795, https://doi.org/10.1002/ente.201900795.

[36] G. Kresse, J. Hafner, Ab initio molecular dynamics for liquid metals, Phys. Rev. B 47 (1993) 558-561, https://doi.org/10.1103/PhysRevB.47.558.

[37] J.P. Perdew, K. Burke, M. Ernzerhof, Generalized Gradient Approximation Made Simple, Phys. Rev. Lett. 77 (1996) 3865-3868, https://doi.org/10.1103/PhysRevLett.77.3865.